

Geometry processing with discrete exterior calculus

Lenka Ptackova^{1,2,3}

¹Instituto Nacional de Matemática Pura e Aplicada (IMPA), Rio de Janeiro, Brazil

²Institute of Computer Science, Universidade Federal do Rio de Janeiro, Brazil

³Department of Numerical Mathematics, Charles University, Czech Republic

6th of March 2025

Work initiated under supervision of Luiz Velho, IMPA

Why (novel) discrete exterior calculus?

- We are interested in geometry processing on **curved surface meshes**.
- **Exterior calculus** is a coordinate-free calculus that greatly simplifies analysis and calculations on curved spaces of differential manifolds.
- **Discrete exterior calculus** (DEC) is a discrete counterpart of exterior calculus on discretized domains (meshes).
- The vast majority of work on DEC is restricted to triangle meshes, despite the **prevalence of non-triangle surface meshes** in geometric design and engineering applications.

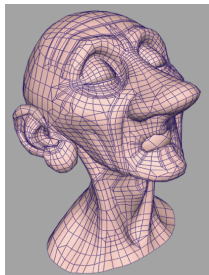


Figure: The control mesh for Geri's head used for recursive Catmull-Clark subdivision. Catmull-Clark subdivision produces meshes consisting only of quadrilaterals. Image taken from [DKT98].

Outline

To expose our framework, published in [Pta17, PV17, PV21], we shall look at:

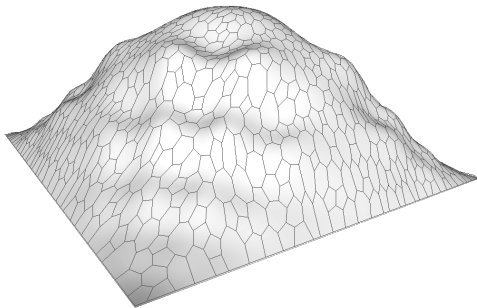
1. Discretization of differential surfaces and discretization of differential forms.
2. Definition of new discrete versions of several operators, including:
 - wedge product,
 - Hodge star operator,
 - codifferential,
 - Laplace–de Rham operator,
 - Lie derivative.
3. Evaluation of accuracy of our operators by series of numerical test.
4. Comparisson to existing related methods.
5. Application of our operators for various tasks such as:
 - mesh smoothing by mean curvature flow,
 - vector field decomposition,
 - Lie advection of functions and vector fields.

A mesh and discrete differential forms

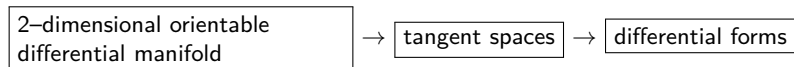
POV of Algebraic Topology ↓



↑
discretization



↑
discretization



POV of Differential Geometry ↑

Discretization of differential manifold

A mesh $M = (F, E, V)$ is a **2-dimensional orientable pseudomanifold**:

- every 0-dimensional cell —vertex $v \in V$ and every 1-dimensional cell —edge $e \in E$ is an element of a 2-dimensional cell $f \in F$;
- every edge $e \in E$ is an element of at most two 2-dimensional cells;
- given any two faces $f_a, f_b \in F$, there exists a sequence of faces $f_a = f_0, f_1, \dots, f_k = f_b$ such that f_{i-1} and $f_i, i = 1, \dots, k$, have a common edge (M is strongly connected cellular complex);
- all faces of f can be oriented such that any pair of faces f_i, f_j sharing an edge e can be oriented coherently, i.e., $[f_i : e] + [f_j : e] = 0$, where $[f : e] \in \{-1, 0, 1\}$ denotes the incidence number of f and e .

A **k -chain** is a function c from the set of oriented k -cells to the integers. We add k -cells to k -chains by adding their values, the resulting group is the chain group $C_k(M)$.

Further, let G be an abelian group, the group of **k -cochains** of M , with coefficients in G , is the group $C^k(M) = \text{Homomorphism}(C_k(M), G)$.

Discretization of differential forms

Let M be a Riemannian manifold and TM a tangent bundle on it. A \mathbb{R} -valued *differential k -form* Ω^k is a smooth antisymmetric k -linear map of a set of k tangent vectors to a scalar, that is:

$$\Omega^k : TM \times \cdots \times TM \rightarrow \mathbb{R}.$$

A differential k -form is also seen as an oriented density that can be integrated over a k -dimensional manifold or k -dimensional chain. Thus (ideal) **discretization of differential forms** reads:

$$\alpha_D^0(v) = \alpha^0(v), \quad \beta_D^1(e) = \int_e \beta^1, \quad \kappa_D^2(f) = \int_f \kappa^2,$$

where $v \in V$, $e \in E$, $f \in F$ of a mesh $M = (V, E, F)$. Furthermore, a vector field X is discretized over an edge $e = (v_0, v_1)$ as a 1-form X_D^b :

$$X_D^b(e) = \int_e \langle e', X \rangle = \int_0^1 \langle e'(t), X(e(t)) \rangle dt, \quad e(t) = v_0 + t(v_1 - v_0), \quad t \in [0, 1].$$

Discretization of differential forms

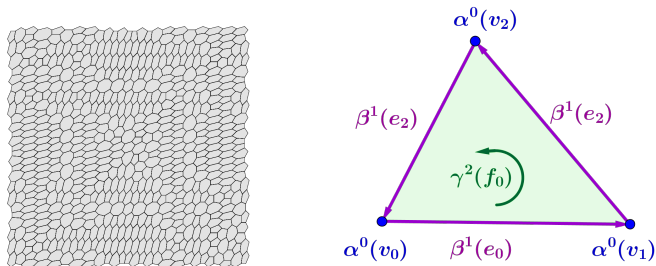


Figure: The mesh on the left shall be used for numerical tests of discrete wedge product. As illustrated in the left figure, we assign discrete 0-forms to vertices, discrete 1-forms to edges, and discrete 2-forms to faces of a mesh.

For example, numerical tests of discrete wedge product are performed with the following differential forms:

$$\begin{aligned}\alpha^0 &= \sin(x) \cos(y) + 1, \\ \beta^1 &= (\sin^2(x) - 1)dx + (3 \cos(x + 2) + \sin(y))dy, \\ \omega^2 &= (\sin(xy) + \cos(1))dx \wedge dy.\end{aligned}$$

Our Approach

- DEC has been well developed for triangle meshes — mainly by computer graphics community, e.g., [Hir03], we call it the **classical DEC**.
- We provide an extension of DEC from triangle to general polygonal meshes on flat and curved surfaces.
- Our approach has several advantages:
 1. Working directly with polygonal meshes bypasses the need for combinatorial subdivision.
 2. Our construction operates solely on primal (input) meshes, thus removing any dependency on dual meshes, unlike in the classical DEC.
 3. Our method allows for discretization of new differential operators such as the Lie derivative.

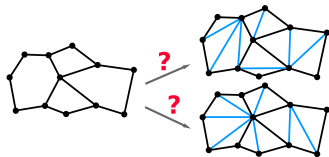
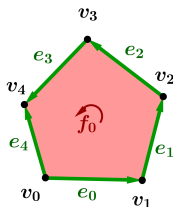


Figure: By working directly with polygonal meshes, we overcome the ambiguities of subdividing a discrete surface into a triangle mesh. Furthermore, we thus store less data.

Discrete Exterior Calculus

We define all operators through these 3 “basic” discrete operators:

1. **Exterior derivative** d (metric independent) – borrowed from algebraic topology: it is the *coboundary operator* of cochains. It satisfies the Stokes’ formula.
2. **Wedge product** \wedge (metric independent) – shares several defining properties with the *cup product* of algebraic topology.
3. **Hodge star operator** \star (metric dependent).



$$[f_0 : e_0] = 1, [f_0 : e_1] = 1, \dots, [f_0 : e_4] = -1$$

$$\partial f_0 = \sum_{e_i \in E} [f_0 : e_i] e_i = e_0 + e_1 + e_2 + e_3 - e_4$$

$$\begin{aligned} d\alpha(f_0) &= \sum_{e_i \in E} [f_0 : e_i] \alpha(e_i) \\ &= \alpha(e_0) + \alpha(e_1) + \dots - \alpha(e_4) \end{aligned}$$

Figure: Exterior derivative d as the coboundary operator. Here ∂ denotes the *boundary operator* and $[f_0 : e_i]$ is the incidence number between face f_0 and edge e_i .

Our Contribution

- We define a new **polygonal wedge product** \wedge compatible with discrete exterior derivative such that it obeys the Leibniz product rule.
- We introduce a novel **primal-to-primal Hodge star operator** \star , that does not involve any dual mesh.
- Using these two operators we derive a **discrete contraction operator** (called also interior product) \mathbf{i}_X .
- The contraction operator together with discrete exterior derivative then allows for definition of the **discrete Lie derivative** $L_X = \mathbf{i}_X d + d \mathbf{i}_X$.
- We also define a discrete version of the **codifferential** δ and **Laplace-de Rham operator** $\Delta = d\delta + \delta d$.

Discrete Wedge Product

- Just like the wedge product of differential forms Ω , our discrete wedge product is a **bilinear operation** such that

$$\wedge : \Omega^k \times \Omega^l \rightarrow \Omega^{k+l}.$$

- Our polygonal wedge product satisfies the **Leibniz product rule** and is **skew-commutative**, just like its differential analog. However, it is **associative** only if one of the 0-forms involved is closed.
- It extends the notion of a **cup product** from simplicial and cubical 2-dimensional pseudomanifolds to general polygonal case.

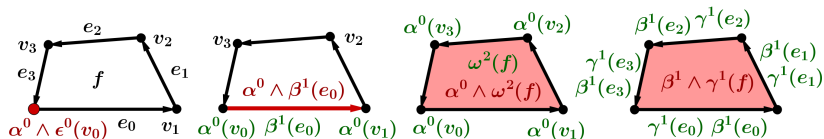


Figure: The wedge product on a quadrilateral: the product of two 0-forms is a 0-form located on vertices (far left). The product of a 0-form with a 1-form is a 1-form located on edges (center left). The product of a 0-form with a 2-form is a 2-form located on faces (center right), and the product of two 1-forms is a 2-form located on faces (far right).

Discrete Wedge Product – Numerical Behavior

Numerical tests on flat and curved surface meshes (possibly with non-planar and non-convex faces) show at least **linear convergence** to the respective analytical solutions, both in L^2 and L^∞ norm.

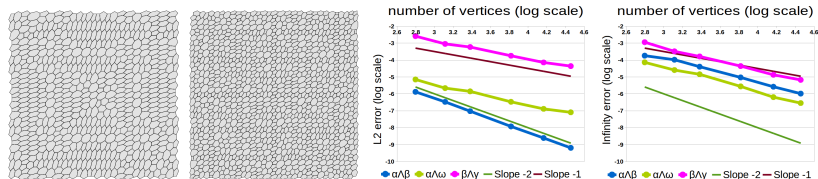


Figure: Convergence of the wedge products on a set of unstructured polygonal meshes on a planar square to analytical solutions in L^2 norm (center right) and L^∞ norm (right). Both axes are in \log_{10} scale. The differential forms tested are: $\alpha^0 = \sin(x) \cos(y) + 1$, $\beta^1 = (\sin^2(x) - 1)dx + (3 \cos(x + 2) + \sin(y))dy$, $\gamma^1 = (\cos(x) \sin(y) + 3)dx + \cos(y)dy$, $\omega^2 = (\sin(xy) + \cos(1))dx \wedge dy$. Two samples of test meshes (left and center left) over a planar $[-1, 1]^2$ square.

Hodge Star Operator

- Discrete Hodge star operator is defined as a linear operator such that

$$\star : \Omega^k \rightarrow \Omega^{2-k}.$$

- Since dual forms are attributed to primal elements, we can compute discrete wedge products of primal and dual forms and define a contraction operator later on.
- On the other hand, there is no isomorphism between the groups of k - and $(2 - k)$ -dimensional cells, in general. Hence our Hodge star **is not an isomorphism**, unlike the Hodge star on Riemannian manifolds.

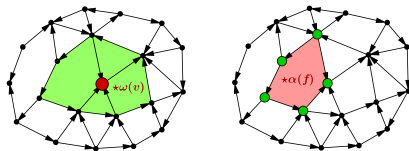


Figure: Left: Hodge dual of a 2-form ω is a 0-form $\star\omega$, whose value on vertex v (colored red) is a linear combination of values of ω on adjacent faces (colored green). Right: Hodge dual of a 0-form α is a 2-form $\star\alpha$, the value of $\star\alpha$ on face f (colored red) is a linear combination of values of α on vertices (green) of that face.

Hodge Star Operator – Numerical Behavior

Numerical tests on flat and curved surface meshes show at least **linear convergence** to the respective analytical solutions, both in L^2 and L^∞ norm.

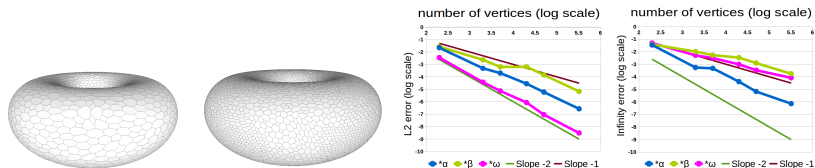


Figure: Test meshes of a torus azimuthally symmetric about the z-axis with 5k vertices (far left) and 20k vertices (center left). Graphs show the approximation errors of the discrete Hodge star on a set of such irregular polygonal meshes on the torus, in L^2 norm (center right) and L^∞ norm (far right). We have chosen $\alpha^0 = x^2 + y^2$, $\beta^1 = X^b$, where $X = (-y, x, 0)$ is a tangent vector field, and $\omega^2 = \mu$ is the area element on the torus. Thus $\star\omega = \star\mu = 1$, $\star\alpha = (x^2 + y^2)\mu$, and $\star\beta = Y^b$, where $Y = 2(-xz, -yz, x^2 + y^2 - \sqrt{x^2 + y^2})$ is a tangent vector field orthogonal to X . Both axes are in \log_{10} scale.

Contraction Operator

The contraction operator maps k -forms to $(k - 1)$ -forms. We define our **discrete contraction operator** \mathbf{i}_X on a polygonal mesh M by the following property that holds on Riemannian 2-manifolds (see [Hir03, Lemma 8.2.1]):

$$\mathbf{i}_X \alpha = (-1)^{k(2-k)} \star (\star \alpha \wedge X^b), \quad \alpha \in C^k(M), \quad k = 1, 2, \quad (1)$$

where X is a tangent vector field and b is (discrete) flat operator that maps vector fields to (discrete) differential forms.

On Riemannian manifolds, it is an *antiderivation*, because it obeys a graded Leibniz rule with wedge product:

$$\mathbf{i}_X(\alpha^k \wedge \beta^l) = (\mathbf{i}_X \alpha^k) \wedge \beta^l + (-1)^k \alpha^k \wedge (\mathbf{i}_X \beta^l).$$

However, in our discrete setting the Leibniz product rule is satisfied only if α or β is a closed 0-form. In [Hir03] the author argued that the Leibniz rule for contraction operator, therefore also for Lie derivative, might not hold due to the discrete wedge product not being associative in general.

Contraction Operator – Numerical Behavior

Our discrete contraction of 2-forms wrt to different vector fields exhibit **linear convergence** to the analytically computed solutions, both in L^∞ and L^2 norms. On 1-forms, the errors of approximation decrease **linearly** in L^2 norm and with **slope** 0.5 in L^∞ norm.

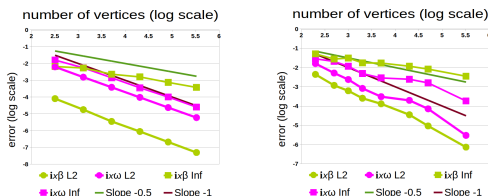
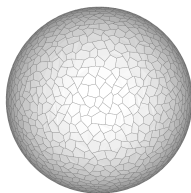


Figure: The contraction operator on a unit sphere (center) and a torus (right). For the sphere we have used the set of jittered with $r = 0.4$ as in the sample mesh (left), and contracted forms $\beta^1 = -xzdx - yzdy + (x^2 + y^2)dz$, $\omega^2 = xdy \wedge dz + ydz \wedge dx + zdx \wedge dy$ wrt vector field $X = (-y, x, 0)$. For the torus we have contracted differential forms $\beta^1 = \mathbb{Y}^b$, $\mathbb{Y} = (-y, x, 0)$, and $\omega^2 = \mu$ wrt vector field $X = 2(-xz, -yz, x^2 + y^2 - \sqrt{x^2 + y^2})$ on the same set of meshes as in the Hodge star operator case. Here $i_X \beta$ L2 denotes the L^2 error approximation of the contraction operator on the 1-form β , whereas $i_X \beta$ Inf denotes the L^∞ error approximation on β , and similarly for the 2-form ω .

Lie Derivative

We define **discrete Lie derivative** $L_X : \Omega^k \rightarrow \Omega^k$ using the Cartan's homotopy formula and our discrete contraction operator:

$$L_X \alpha = \mathbf{i}_X d\alpha + d\mathbf{i}_X \alpha, \quad \alpha \in \Omega^k(M), \quad k = 0, 1, 2, \quad X \in TM. \quad (2)$$

The Lie derivative is the directional derivative of a k -form α in the direction X . It measures the rate of change of α along of the flow generated by vector field X .

Lie Derivative – Numerical Behavior

The Lie derivatives exhibit **converging behavior** on regular meshes, planar and non-planar. However, the L^2 error of approximation of Lie derivatives of 1- and 2-forms on irregular meshes stays rather **constant**.

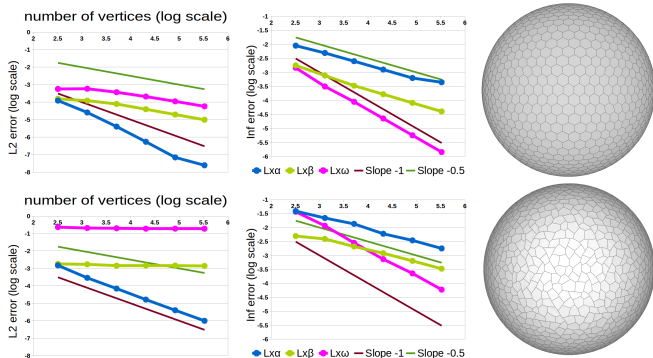


Figure: Influence of jittering on experimental convergence of discrete Lie derivatives: L^2 and L^∞ errors on a set of regular polygonal meshes on a sphere (upper row) and jittered meshes with vertex displacement by $0.4 \times$ shortest edge length (lower row). Here $\alpha^0 = x^2 + y^2$, $\beta^1 = Y^b$, where $Y = 2(-xz, -yz, x^2 + y^2 - \sqrt{x^2 + y^2})$, $\omega^2 = xdy \wedge dz + ydz \wedge dx + zdx \wedge dy$, and $X = (-y, x, 0)$.

The Codifferential and Laplacian

Just like on Riemannian n -manifolds M , the Hodge star operator is employed to define **codifferential operator** $\delta : \Omega^k(M) \rightarrow \Omega^{k-1}(M)$ by

$$\delta(\alpha^k) = (-1)^{n(k-1)+1} \star d \star \alpha.$$

Then using the codifferential operator, the **Laplace–de Rham operator** is given as

$$\Delta := \delta d + d\delta.$$

In [AW11], we find a codifferential operator acting on 1-forms and Laplacian acting on 0-forms on general polygonal meshes given as

$$\delta_1 = M_0^{-1} d_0^\top M_1, \quad L_0 = M_0^{-1} d_0^\top M_1 d_0,$$

where M_0 and $M_1 = M_f + \lambda C_f C_f^\top$ for *admissible* matrix C_f are defined in [AW11, eq. (9), (10)]. We compare our operators with theirs next.

The Codifferential Operator – Numerical Behavior

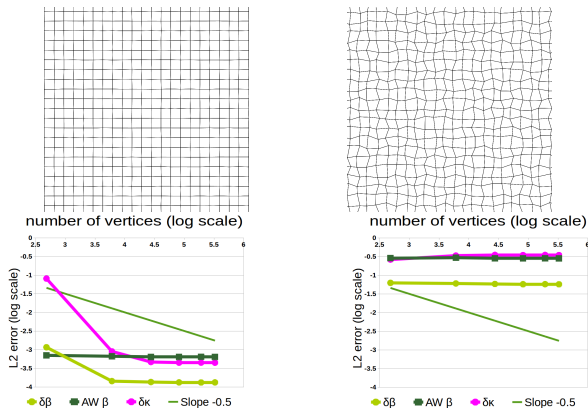


Figure: The influence of jittering on experimental convergence of codifferentials of a 1-form $\beta^1 = (\sin(2x) + \cos(\frac{1}{2}))dx + (3\sin(x) - \cos(y))dy$ and a 2-form $\kappa^2 = (\sin(4x + 4) + \cos(1 - 3y))dx \wedge dy$ on a set of planar quadrilateral jittered meshes with vertex displacement $0.01 \times$ shortest edge length (L) and $0.2 \times$ shortest edge length (R). Here $AW\beta$ stands for the L^2 error of approximation of the codifferential of [AW11] with $\lambda = 0$.

The Laplacian – Numerical Behavior

Our Laplace operator on 0-forms is **linearly precise**, i.e., it is zero on linear forms in the plane.

The experimental convergence of our discrete Laplacian is comparable to convergence of *purely geometric Laplacian* of [AW11], but the error of approximation is smaller than for their *combinatorially enhanced Laplacians*.

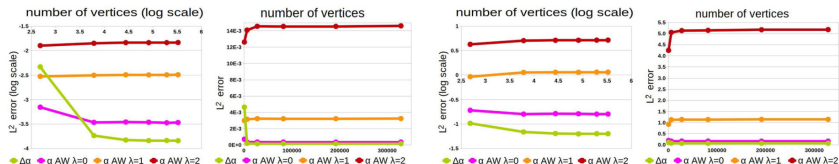


Figure: Discrete Laplacians of 0-form $\alpha = \sin(x - 1) - \cos(2y)$ on sets of planar quadrilateral jittered meshes with vertex displacement $0.01 \times$ shortest edge length (far and center left) and $0.2 \times$ shortest edge length (center and far right). Note that the graphs in the center left and on the far right are in arithmetic scale. Here $AW\alpha$ stands for the L^2 error of approximation of the Laplacians of [AW11] with $\lambda = 0, 1, 2$, see [AW11, section 3.3].

Applications: Implicit mean curvature flow

If f is a 0-form representing coordinates of points on a smooth surface M in \mathbb{R}^3 , then

$$\Delta f = -\vec{H}(f),$$

where $\vec{H}(f)$ is the mean curvature vector at point $f \in M \setminus \partial M$.

Let V_0 be vertex positions of an initial mesh M , we move its interior vertices along mean curvature flow to decrease the curvature. Concretely, we employ backward Euler method and solve the following linear system:

$$(I + dt\Delta)V_{k+1} = V_k, \quad k \geq 0, \quad dt > 0.$$

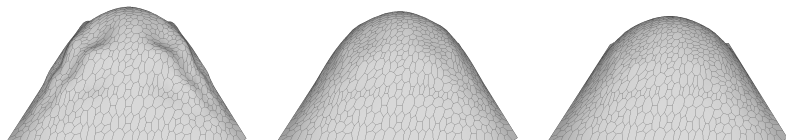


Figure: Discrete mean curvature flow with time step $dt = 0.02$ on a general polygonal mesh with 2399 vertices: initial mesh (L), mesh after one (C) and two iterations (R). We fixed the boundary vertices.

Applications: Implicit mean curvature flow

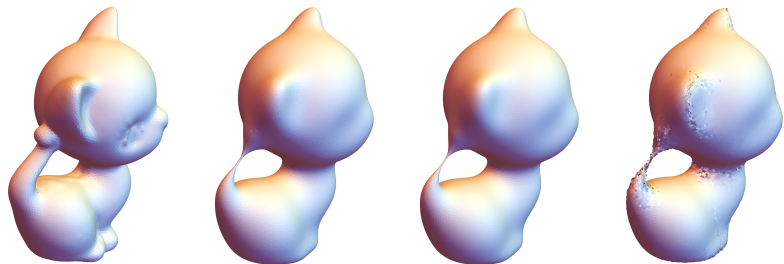


Figure: Comparison of implicit mean curvature flows on a general polygonal mesh (29k vertices) after 10 iterations with time step $t = 10^{-4}$. The original mesh (left), mesh smoothed by our method (center left). The algorithm of [AW11] with $\lambda = 1$ (center right) produces a visually well-smoothed meshes. However, their method with $\lambda = 0$ (right) exhibits some undesirable artifacts on the ears, neck, and tail of the kitten.

Applications: Discrete Helmholtz–Hodge Decomposition

The Hodge theorem states that a differential k -form ω on an oriented compact Riemannian manifold without boundary can be uniquely decomposed into three parts

$$\omega = d\alpha + \delta\beta + \gamma \quad (3)$$

for some $(k - 1)$ -form α , $(k + 1)$ -form β , and a harmonic k -form γ ($\Delta\gamma = 0$).

If we decompose a vector field as a differential 1-form ω^1 , then

1. $d\alpha$ corresponds to a curl-free component of the vector field,
2. $\delta\beta$ corresponds to a divergence-free (incompressible) component,
3. γ corresponds to a harmonic component.

This is the **three component form** of the HHD. As mentioned in [Bhatia et al. 2013], some applications employ the **two component form** of the HHD, where the harmonic component is "included" either into the curl-free or the divergence-free part.

Applications: Discrete Helmholtz–Hodge Decomposition



Figure: Original vector field (left), its incompressible component (center) and its curl-free component (right).

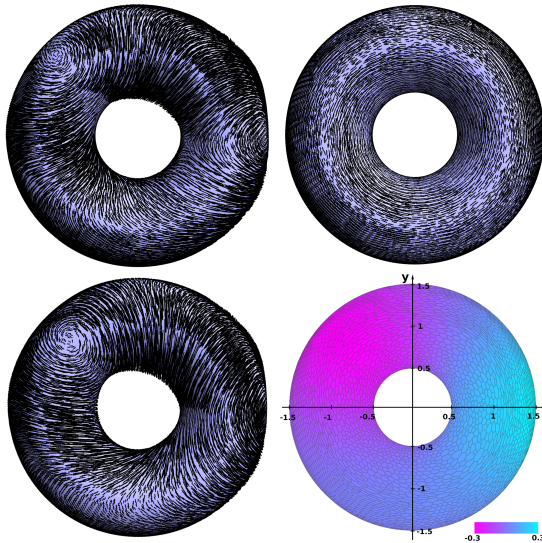


Figure: HHD of an incompressible vector field X (top left) on a torus (mesh with 20k vertices). The original vector field is $X = X_H + X_R$, where $X_H = (-y, x, 0)$ is a harmonic field, and X_R is a rotational vector field. Our discrete decomposition gives approximate expected results. The calculated decomposition consists of harmonic part γ^\sharp (top right) and rotational part $(\delta\beta)^\sharp$ (bottom left). We also depict vector potential β in pseudocolors (bottom right). The potential of strongest CCW rotation is cyan, CW rotation is magenta.

Applications: Lie Advection

We can model advection of a conserved q -form β in a flow generated by vector field X by solving the Lie advection equation:

$$\frac{\partial \beta}{\partial t} + L_X \beta = 0.$$

Thus to advect a discrete q -form β by the flow of a vector field X , we can iterate over discrete solutions using a simple forward Euler method:

$$\beta_{k+1} = \beta_k - dt L_X \beta_k, \quad k = 0, \dots, \quad (4)$$

where dt is the time step, k is the number of iterations.

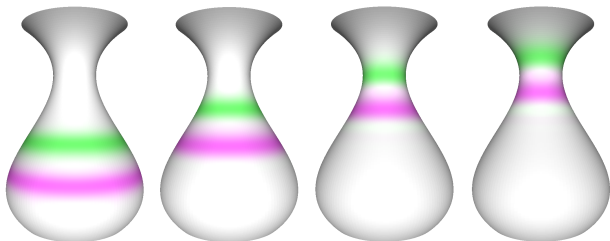


Figure: Lie advection of a color function (a (R,G,B)-valued 0-form) on a mesh of a vase.

Applications: Lie Advection

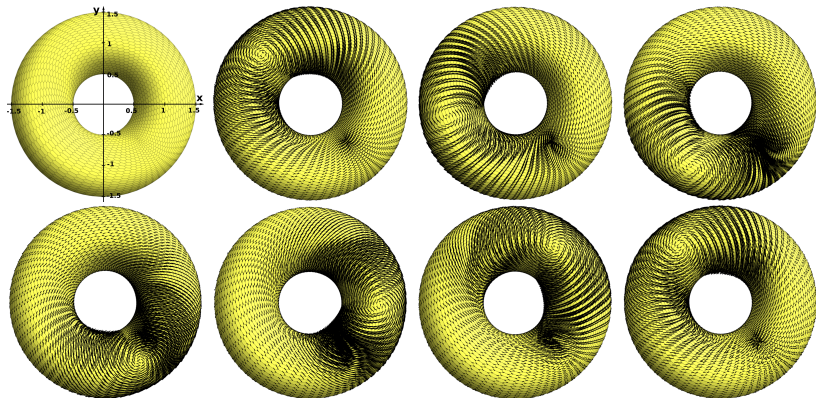


Figure: Lie advection on a mesh on torus with 8k vertices (top left corner). We advect a vortical tangent vector field Y_0 (second picture from the left) along the flow of a harmonic tangent vector field $X = (-y, x, 0)$. We apply time steps of length 10^{-3} . From left to right and top to bottom, we plot the advected vector field Y_k after 1000, 2000, \dots , 5000 iterations and at the bottom right after 6283 iterations. Since the flow is periodic, Y_k should be equal to original state Y_0 for $k = 2\pi \cdot 10^3 \approx 6283$.

Discussion

- Geometry processing on general polygonal meshes is getting more attention in last few years, especially within computer graphics community, see [DGBD20, BBW⁺24] and references therein.
- We have presented a novel framework for geometry processing on general polygonal meshes as a new discrete version of Exterior Calculus, that allowed for definition of Lie derivative.
- Contrary to the so called Polygonal Laplacian [BBW⁺24], **Lie derivative** has not yet been explored enough, especially on polygonal meshes.
- Experimental convergence of Lie derivative was observed on regular meshes, however on irregular meshes the L^2 error of approximation kept rather constant.
- Our discrete Laplace operator is numerically comparable to the purely geometric Laplacian of [AW11], but results in a better mesh smoothing. On the other hand, our Laplacian gives a better numerical approximation of the analytically computed Laplacian than their combinatorially enhanced Laplacians, yet performs as well as theirs in mesh smoothing.

Future and Ongoing Work

- Apply Schwarz domain decomposition methods in geometry processing tasks in combination with our framework.
- Compare our Laplacian to newly emerged polygonal Laplacians ([BBW⁺24] and references therein).
- Analyze with greater details algebraic properties of our operators and establish under what conditions they meet the algebraic properties of operators on differential manifolds.
- Apply our framework for 2D fluid flow simulation and compare our method to traditional methods (FVM) used in computational fluid dynamics, since Navier–Stokes equation can be rewritten in terms of differential forms, see [WIL11, MHS16].
- Examine the possibility of extending DEC to 3–dimensional manifolds, such as volumetric meshes made of tetrahedrons or 3–dimensional (topological) cubes. See [Arn12] for treatment of cubical complexes.

References I

-  Rachel F. Arnold, *The discrete hodge star operator and poicare duality*, Ph.D. thesis, Virginia Tech, 2012.
-  Marc Alexa and Max Wardetzky, *Discrete laplacians on general polygonal meshes*, ACM Trans. Graph. **30** (2011), no. 4.
-  A. Bunge, D. R. Bukenberger, S. D. Wagner, M. Alexa, and M. Botsch, *Polygon laplacian made robust*, Computer Graphics Forum **43** (2024), no. 2, e15025.
-  Fernando De Goes, Andrew Butts, and Mathieu Desbrun, *Discrete differential operators on polygonal meshes*, ACM Trans. Graph. **39** (2020), no. 4.
-  Tony DeRose, Michael Kass, and Tien Truong, *Subdivision surfaces in character animation*, SIGGRAPH '98, p. 85–94, Association for Computing Machinery, New York, NY, USA, 1998.
-  Anil Nirmal Hirani, *Discrete exterior calculus*, Ph.D. thesis, California Institute of Technology, 2003.

References II

-  Mamdouh S. Mohamed, Anil N. Hirani, and Ravi Samtaney, *Discrete exterior calculus discretization of incompressible navier–stokes equations over surface simplicial meshes*, Journal of Computational Physics **312** (2016), 175–191.
-  Lenka Ptackova, *Discrete wedge product on polygonal pseudomanifolds*, Ph.D. thesis, IMPA, Rio de Janeiro, Brazil, 2017.
-  Lenka Ptackova and Luiz Velho, *A primal-to-primal discretization of exterior calculus on polygonal meshes*, Proceedings of the Symposium on Geometry Processing: Posters (Goslar, DEU), SGP '17, Eurographics Association, 2017, p. 7–8.
-  Lenka Ptackova and Luiz Velho, *A simple and complete discrete exterior calculus on general polygonal meshes*, Computer Aided Geometric Design **88** (2021), 102002.



SCOTT O. WILSON, *Differential forms, fluids, and finite models*,
Proceedings of the American Mathematical Society **139** (2011),
no. 7, 2597–2604.